Analysis of Magnetic Particle Capture in the Microvasculature

E. P. Furlani, K. C. Ng, and Y. Sahoo

The Institute for Lasers, Photonics, and Biophotonics, University at Buffalo SUNY
432 Natural Science Complex
Buffalo, NY 14260-3000
efurlani@buffalo.edu, ysahoo@buffalo.edu

ABSTRACT

A model is presented for predicting the capture of therapeutic magnet nanoparticles in the microvasculature. The particles are functionalized with surface-bound anticancer agents and directed to malignant tissue using an applied magnetic field. The model takes into account the dominant magnetic and fluidic forces on the particles. The magnetic force is predicted using a linear magnetization model for the magnetic response of the particles. The fluidic force is based on Stokes' law wherein the blood viscosity is determined using an empirically-based analytical expression that accounts for blood flow in the microvasculature. The model is demonstrated for a noninvasive magnetic targeting system. The equations of motion are solved numerically to predict particle transport and capture for this system, and the analysis demonstrates the viability of using noninvasive magnetophoretic control to effect drug delivery to tumors that are within a few centimeters of the field source. The model presented here enables rapid parametric analysis of system performance, and is well-suited for the optimization of invasive or noninvasive drug delivery systems.

Keywords: magnetophoresis, magnetic drug targeting, magnetophoretic particle capture, drug targeting in microvasculature, *in vivo* drug targeting

1 INTRODUCTION

Magnetophoretic targeting of malignant tissue using anticancer agents bound to magnetic carrier particles has the potential to improve the effectiveness of anticancer treatment while reducing deleterious side effects. There is growing interest in this therapy due to rapid progress in the development of therapeutic magnetic nanoparticles that are custom tailored to target a specific tissue, and effect local chemo-, radio- and gene therapy at a tumor site [1]. In magnetic drug targeting, magnetic carrier particles with surface-bound drug molecules are injected into the vascular system, upstream from malignant tissue, and captured at the tumor using an applied magnetic field. Figure 1 illustrates an example of noninvasive targeting in which the field source is positioned outside the body.

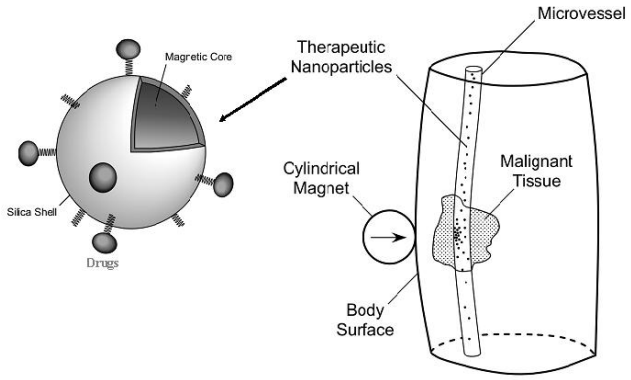

Figure 1: Noninvasive Magnetic Drug Targeting.

In this article we present a model for predicting magnetic targeting of therapeutic mico/nano-particles in the microvasculature. We demonstrate the model by applying it to the system shown in Fig 1. Here, the applied field is provided by a rare-earth cylindrical magnet that is magnetized perpendicular to its axis. The magnet is assumed to be of infinite extent, with an orientation that is orthogonal to the microvessel (Figs. 1 and 2). We use analytical expressions for the dominant magnetic and fluidic forces. The magnetic force is obtained using a well-known field solution for the magnet combined with a linear magnetization model for the magnetic response of the particles. The fluidic force is based on the assumption of laminar blood flow through a cylindrical microvessel, and the blood rheology is taken into account using an empirically-based formula for the effective blood viscosity. We use the force expressions in the equations of motion, which are solved numerically to predict particle trajectories within the microvessel. The analysis demonstrates the viability of using noninvasive magnetophoretic control to effect targeted delivery of therapeutic drugs to tumors that are within a few centimeters from the field source. The model presented here can be adapted to a variety of targeting systems, both invasive and noninvasive, and is ideal for parametric optimization of magnetic drug delivery systems.

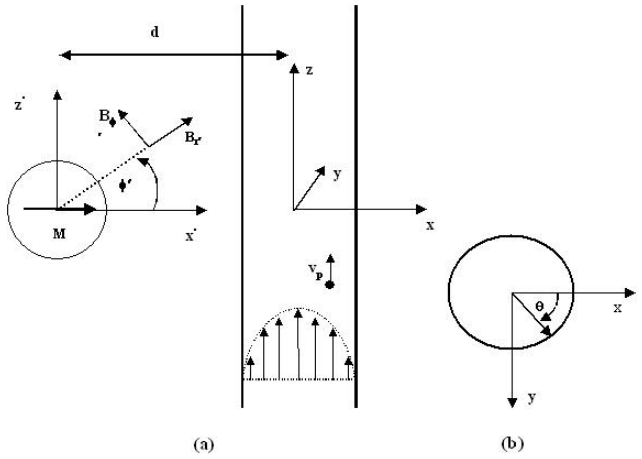

Figure 2: Reference Frame for Analysis.

2 THEORETICAL MODEL

Magnetic particle transport in the microvasculature is governed by several factors including (a) the magnetic force due to an applied field, (b) the fluidic drag force, (c) particle/blood-cell interactions (blood rheology), (d) inertia, (e) buoyancy, (f) gravity, (g) thermal kinetics (Brownian motion), (h) particle/fluid interactions (perturbations to the flow field), and (i) interparticle effects such as magnetic dipole-dipole interactions. In this paper, we take into account the dominant magnetic and fluidic forces, and particle/blood-cell interactions via an effective blood viscosity that is a function of the diameter of the blood vessel and the level of hematocrit.

We predict particle transport using Newton's law,

$$\mathrm{m_p}\frac{\mathrm{d}\mathbf{v}_\mathrm{p}}{\mathrm{dt}} = \mathbf{F}_\mathrm{m} + \mathbf{F}_\mathrm{f}, \tag{1}$$

where $\mathrm{m_p}$ and $\mathbf{v}_\mathrm{p}$ are the mass and velocity of the particle, and $\mathbf{F}_\mathrm{m}$ and $\mathbf{F}_\mathrm{f}$ are the magnetic and fluidic forces respectively. The magnetic force is given by

$$\mathbf{F}_\mathrm{m} = \mu_0 \mathrm{V_p}\left(\mathbf{M}_\mathrm{p} \bullet \nabla\right)\mathbf{H}_\mathrm{a}, \tag{2}$$

where $\mathrm{V_p}$ and $\mathbf{M}_\mathrm{p}$ are the volume and magnetization of the particle, and $\mathbf{H}_\mathrm{a}$ is the applied magnetic field intensity inside the particle (we use the value at the center of the particle). The fluidic force is obtained using the Stokes' approximation for the drag on a sphere

$$\mathbf{F}_\mathrm{f} = -6\pi\eta \mathrm{R_p}(\mathbf{v}_\mathrm{p} - \mathbf{v}_\mathrm{f}), \tag{3}$$

where η and $\mathbf{v}_\mathrm{f}$ are the viscosity and the velocity of the fluid, respectively.

The Newtonian approach does not take into account Brownian motion, which can influence particle capture when the particle diameter $\mathrm{D_p}$ is sufficiently small. Gerber et al. [2] have developed the following criterion to estimate this diameter

$$\left|\mathrm{F}\right| \mathrm{D_p} \le kT, \tag{4}$$

where $\left|\mathrm{F}\right|$ is the magnitude of the total force acting on the particle, k is Boltzmann's constant, and T is the absolute temperature. For particles with a diameter below this value one solves an advection-diffusion equation for the particle concentration c, rather than the Newtonian equation for the trajectory of a single particle. The concentration is governed by the following equation [2],

$$\frac{\partial c}{\partial t} + \nabla \bullet \mathbf{J} = 0,, \tag{5}$$

where $\mathbf{J} = \mathbf{J}_D + \mathbf{J}_F$ is the total flux of particles, which includes a contribution $\mathbf{J}_D = -D\nabla c$ due to diffusion, and a contribution $\mathbf{J}_F = \mathbf{v}c$ due to the action of all external forces. The diffusion coefficient D is given by the Nernst-Einstein relation $D = \mu kT$, where $\mu = 1/(6\pi\eta R_p)$ is the mobility of a particle of radius R_p in a fluid with viscosity η (Stokes' approximation). The drift velocity also depends of the mobility $\mathbf{v} = \mu\mathbf{F}$, where $\mathbf{F} = \mathbf{F}_\mathrm{m} + \mathbf{F}_\mathrm{f} + \cdots$ is the total force on the particle.

2.1 Magnetic Force

Consider the noninvasive targeting system shown in Figs. 1 and 2. The magnet has a radius R_{mag} and is centered with respect to the origin in the x'-z' plane as shown in Fig. 2. The magnet is magnetized to a level M_s perpendicular to its axis. The field solution for this structure is well-known, and its field components in cylindrical coordinates are (p. 179 of [3])

$$\mathrm{H}_r(r',\phi') = \frac{\mathrm{M_s}}{2}\frac{R_{mag}^2}{r'^2}\cos(\phi'), \tag{6}$$

and

$$\mathrm{H}_r(r',\phi') = \frac{\mathrm{M_s}}{2}\frac{R_{mag}^2}{r'^2}\sin(\phi'). \tag{7}$$

To determine the magnetic force, we need an expression for the magnetic response of the particles. We use a linear magnetization model with saturation in which

$$\mathbf{M}_\mathrm{p} = f(\mathrm{H}_\mathrm{a})\mathbf{H}_\mathrm{a}, \tag{8}$$

where

$$f(\mathrm{H_a})=\begin{cases}\dfrac{3(\chi_\mathrm{p}-\chi_\mathrm{f})}{(\chi_\mathrm{p}-\chi_\mathrm{f})+3} & \mathrm{H_a}<\left(\dfrac{(\chi_\mathrm{p}-\chi_\mathrm{f})+3}{3(\chi_\mathrm{p}-\chi_\mathrm{f})}\right)\mathrm{M_{sp}}\\ \mathrm{M_{sp}}/\mathrm{H_a} & \mathrm{H_a}\geq\left(\dfrac{(\chi_\mathrm{p}-\chi_\mathrm{f})+3}{3(\chi_\mathrm{p}-\chi_\mathrm{f})}\right)\mathrm{M_{sp}}\end{cases}. \quad (9)$$

$\mathrm{M_{sp}}$ is the saturation magnetization of the particle, and χ_p and χ_f are the susceptibilities of the particle and fluid respectively [4]. We evaluate the force components in the (x,y,z) coordinates centered with respect to the microvessel (Fig. 2) and obtain

$$\mathrm{F}_{mx}=-\mu_0\mathrm{V_p}f(\mathrm{H_a})\mathrm{M}_s^2R_{mag}^4\frac{(x+d)}{2((x+d)^2+z^2)^3}, \quad (10)$$

and

$$\mathrm{F}_{mz}=-\mu_0\mathrm{V_p}f(\mathrm{H_a})\mathrm{M}_s^2R_{mag}^4\frac{z}{2((x+d)^2+z^2)^3}. \quad (11)$$

The component F_{mx} governs particle capture and from Eq. (10) we find that it is always attractive (towards the magnet) because $d >> x$.

2.2 Fluidic Force

We assume fully developed laminar flow in the blood vessel with the flow velocity parallel to the z-axis, which is defined by a velocity distribution

$$\mathrm{v_f}(x,y)=2\overline{\mathrm{v}}_\mathrm{f}\left(1-\left(\frac{(x^2+y^2)^{1/2}}{R_\mathrm{v}}\right)^2\right) \quad (12)$$

where $\overline{\mathrm{v}}_\mathrm{f}$ is the average fluid velocity in a microvessel of radius R_v. Thus, the fluidic force components are

$$\mathbf{F}_\mathrm{fx}=-6\pi\eta R_p\mathrm{v_x}, \quad (13)$$

$$\mathbf{F}_\mathrm{fy}=-6\pi\eta R_p\mathrm{v_y}, \quad (14)$$

and

$$\mathbf{F}_\mathrm{fz}=-6\pi\eta R_p\left[\mathrm{v_z}-2\overline{\mathrm{v}}_\mathrm{f}\left(1-\left(\frac{(x'^2+y'^2)^{1/2}}{R_v}\right)^2\right)\right]. \quad (15)$$

2.3 Effective Viscosity

To evaluate Eqs. (13) - (15) we need an expression for blood viscosity η. Blood is a suspension of red and white blood cells (erythrocytes and leukocytes), and platelets in plasma. Blood plasma (absent the cells and platelets) is an incompressible Newtonian fluid with a viscosity $\eta_{plasma}=0.0012\ \mathrm{N\cdot s/m^2}$. Red blood cells, when unperturbed, have a biconcave discoid shape with a diameter of 6-8 μm, and a thickness of 2 μm. These cells account for approximately 99% of the particulate matter in blood. The hematocrit, which is the percentage by volume of packed red blood cells in a given sample of blood, is nominally 40-45%. The rheological properties of blood in the microvasculature depend on many factors including the diameter of the blood vessel, the flow velocity, the hematocrit, the finite size of the blood cells, their elastic properties, the aggregation and deformation of the blood cells, etc. We use an analytical empirically-based expression for the in vivo viscosity η, which applies for medium to high shear rates

$$\mathrm{v_f}/D>50/s. \quad (16)$$

Specifically, the apparent blood viscosity (relative to that of plasma) can be estimated using [5].

$$\eta_{rel}=\left[1+(\eta_{0.45}-1)\frac{(1-H_D)^C-1}{(1-0.45)^C-1}\left(\frac{D}{D-1.1}\right)^2\right]\left(\frac{D}{D-1.1}\right)^2. \quad (17)$$

In Eq. (17), D is the diameter of the vessel in microns, $\mathrm{H_D}$ is the hematocrit (normally 0.45), and

$$\eta_{0.45}=6\cdot e^{-0.085D}+3.2-2.44e^{-0.06D^{0.645}}, \quad (18)$$

and

$$C=\left(0.8+e^{-0.075D}\right)\cdot\left(\frac{1}{1+10^{-11}\cdot D^{12}}-1\right)+\frac{1}{1+10^{-11}\cdot D^{12}}. \quad (19)$$

Equation (17) gives the viscosity relative to that of the plasma. Thus, the effective blood viscosity η in Eqs. (13) - (15) is given by

$$\eta=\eta_{rel}\,\eta_{plasma}. \quad (20)$$

3 RESULTS

We demonstrate the model via application to noninvasive drug targeting using magnetite (Fe_3O_4) nanoparticles. Fe_3O_4 particles are biocompatible, and have the following material properties: $\rho_p=5000\ \mathrm{kg/m^3}$, and $\mathrm{M}_{sp}=4.78\times10^5\ \mathrm{A/m}$. The magnetization function (9) for these particles reduces to

$$f(\mathrm{H_a})=\begin{cases}3 & \mathrm{H_a}<\mathrm{M_{sp}}/3\\ \mathrm{M_{sp}}/\mathrm{H_a} & \mathrm{H_a}\geq\mathrm{M_{sp}}/3\end{cases}. \quad (21)$$

We first compute the magnetic force along the axis of the microvessel for $-4R_{mag}\leq z\leq 4R_{mag}$. We use a rare-earth NdFeB magnet, 5 cm in diameter (R_{mag} = 2.5 cm), with a magnetization $\mathrm{M}_s=8\times10^5\ \mathrm{A/m}$ ($\mathrm{B}_r=1.0\ \mathrm{T}$). The magnet is positioned 2.5 cm from the axis of the microvessel (d = 5 cm in Fig. 2). The force is computed on a Fe_3O_4 particle 0.5 μm in diameter ($\mathrm{R_p}$ = 250 nm). Plots of F_{mx} and F_{my}, along with corresponding data obtained using finite element analysis (FEA), are shown in Fig. 3. The vertical force F_{mx}, which is responsible for particle

capture, is always negative (attractive towards the magnet), and is strongest immediately above the center of the magnet ($z / R_{mag} = 0$). The horizontal force F_{mz} peaks at the edges ($z / R_{mag} = \pm 1$), and alternates in sign from one edge to the other. Thus, as a particle moves horizontally above the magnet it experiences a horizontal acceleration as it passes the leading edge of the magnet, followed by a deceleration as it passes the trailing edge. F_{mz} is relatively small and insufficient to hold the particle in place against the fluid force, even at the edge of the microvessel. Nevertheless, we assume that a particle is captured once it contacts the inner wall of the microvessel due to the action of adhesive forces, and the influence of the normal magnetic force.

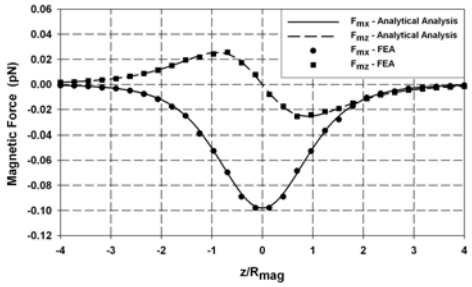

Figure 3: Magnetic force components on a Fe_3O_4 nanoparticle (● = FEA).

We study particle transport through a microvessel with a radius R_v = 50 μm and an average flow velocity $\overline{v}_f = 10$ mm/s. We assume that the hematocrit is 45% and compute the viscosity using (17)-(20) with $\eta_{plasma} = 0.0012$ N·s/m^2. We use the same magnet as above, positioned 15 mm from the microvessel (d = 4 cm in Fig. 2). The particle has a radius R_p = 200 nm and starts upstream at $z(0) = -4R_{mag}$ where the magnetic force is negligible. The initial velocity equals the on-axis flow velocity (i.e., $v_x(0) = 0$, $v_y(0) = 0$, and $v_z(0) = 2\overline{v}_f = 20$ mm/s). We compute the trajectory of the particle as a function of its initial height in the microvessel. Specifically, we numerically integrate Eq. (1) using a fourth-order Runge-Kutta method, and compute a series of trajectories with $x(0)$ = 0, ±0.2R_v, ±0.4R_v, ±0.6R_v, ±0.8R_v and $y(0) = 0$ (Fig. 4). The analysis shows that particles that start at $x(0) \le 0.2R_v$ will be captured, while those starting higher (i.e. farther from the magnetic) will not. We consider 100% capture efficiency to occur when all particles are captured, and we compute the minimum particle radius required to achieve this by setting $x(0) = R_v$. A plot of the minimum particle radius required for 100% capture efficiency as a function of the distance from the magnet to the microvessel is shown in Fig. 5. As expected, larger particles are required to target tissue farther from the magnet (i.e. deeper in the body cavity).

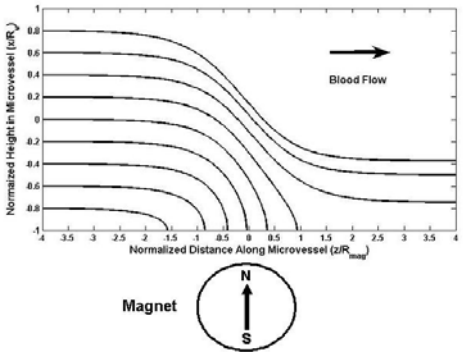

Figure 4: Particle trajectory vs. initial height in microvessel.

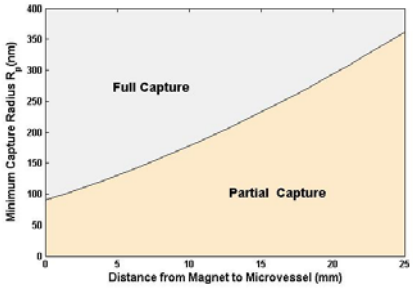

Figure 5: Minimum particle radius required for 100% capture efficiency vs. distance from the magnet.

4 CONCLUSION

A model has been presented for analyzing magnetic drug targeting in the microvasculature. This model enables rapid parametric analysis of drug targeting systems for research and clinical applications.

REFERENCES

[1] F. Marcucci and F. Lefoulon "Active targeting with particulate drug carriers in tumor therapy: fundamentals and recent progress," *Drug Disc. Today* **9** (5) 219-228 2004.

[2] R. Gerber, M. Takayasu , and F. J. Friedlander, "Generalization of HGMS theory: the capture of ultra-fine particles," IEEE Trans. Magn. **19** (5), 2115-2117 1983.

[3] E. P. Furlani, *Permanent Magnet and Electromechanical Devices; Materials, Analysis and Applications*, Academic Press, NY, 2001.

[4] E. P. Furlani, "Analysis of Particle Transport in a Magnetophoretic Microsystem," J. Appl. Phys. **99**, 2006.

[5] A. R. Pries, T.W. Secomb, and P. Gaehtgens, "Biophysical Aspects of Blood Flow Through the Microvasculature," Cardiovasc. Res. **32** 654-667, 1996.